



Missouri University of Science and Technology  
Scholars' Mine

International Specialty Conference on Cold-Formed Steel Structures

Wei-Wen Yu International Specialty Conference on Cold-Formed Steel Structures 2018

Nov 7th, 12:00 AM - Nov 8th, 12:00 AM

## Experimental and Analytical Studies of Cold-Formed Steel Sections with Edge-Stiffened Circular Holes Subjected to Web Crippling

Asraf Uzzaman

James B. P. Lim

David Nash

Amir M. Yousefi

Benjamin Young

Follow this and additional works at: <https://scholarsmine.mst.edu/isccss>

 Part of the [Structural Engineering Commons](#)

### Recommended Citation

Uzzaman, Asraf; Lim, James B. P.; Nash, David; Yousefi, Amir M.; and Young, Benjamin, "Experimental and Analytical Studies of Cold-Formed Steel Sections with Edge-Stiffened Circular Holes Subjected to Web Crippling" (2018). *International Specialty Conference on Cold-Formed Steel Structures*. 7.  
<https://scholarsmine.mst.edu/isccss/24iccfss/session2/7>

This Article - Conference proceedings is brought to you for free and open access by Scholars' Mine. It has been accepted for inclusion in International Specialty Conference on Cold-Formed Steel Structures by an authorized administrator of Scholars' Mine. This work is protected by U. S. Copyright Law. Unauthorized use including reproduction for redistribution requires the permission of the copyright holder. For more information, please contact [scholarsmine@mst.edu](mailto:scholarsmine@mst.edu).

Wei-Wen Yu International Specialty Conference on Cold-Formed Steel Structures  
St. Louis, Missouri, U.S.A., November 7 & 8, 2018

**EXPERIMENTAL AND ANALYTICAL STUDIES OF COLD-FORMED  
STEEL SECTIONS WITH EDGE-STIFFENED CIRCULAR HOLES  
SUBJECTED TO WEB CRIPPLING**

Asraf Uzzaman<sup>1</sup>, James B.P Lim<sup>2</sup>, David Nash<sup>3</sup>, A.M. Yousefi<sup>4</sup> and Ben Young<sup>5</sup>

**Abstract**

Cold-formed steel sections are often used as wall studs or floor joists and such sections often include web holes for ease of installation of services. The holes are normally punched or bored and are unstiffened; when the holes are near to points of concentrated load, web crippling can be the critical design consideration. Recently, a new generation of cold-formed steel channel sections with edge-stiffened circular holes has been developed. The web holes are stiffened through a continuous edge stiffener/lip around the perimeter of the hole. In this paper, a combination of experimental investigations and non-linear finite element analyses are used to investigate the effect of such edge-stiffened holes under the interior-one-flange (IOF) and end-one-flange (EOF) loading conditions; for comparison, sections without holes and with unstiffened holes are also be considered. A non-linear finite element models are described, and the results compared against the laboratory test results; a good agreement was obtained in terms of both strength and failure modes.

Keywords: Cold-formed steel; Web crippling; Finite element analysis; Web openings; Channel section;

---

<sup>1</sup>Research Associate, Department of Mechanical and Aerospace Engineering, The University of Strathclyde, Glasgow, UK

<sup>2</sup> Lecturer, Department of Civil and Environmental Engineering, University of Auckland, New Zealand

<sup>3</sup> Professor, Department of Mechanical and Aerospace Engineering, The University of Strathclyde, Glasgow, UK

<sup>4</sup> PhD Student, Department of Civil and Environmental Engineering, University of Auckland, New Zealand

<sup>5</sup> Professor, Department of Civil Engineering, The University of Hong Kong, Pokfulam Road, Hong Kong.

## 1. Introduction

Cold-formed steel sections are increasingly used in residential and commercial construction for both primary and secondary framing members. Such thin-walled sections are well-known to be susceptible to web crippling, particularly at points of concentrated load or reaction (Rhodes and Nash, 1998). Furthermore, openings in the web are often used to allow ease of installation of electrical or plumbing services. Such openings, however, result in the sections being more susceptible to web crippling, particularly when concentrated loads are applied near to the openings.

Web holes in cold-formed steel sections are normally punched or bored and so are unstiffened (see Fig.1 (a)). Recently, Yu (2012) described a study on a new generation of cold-formed steel channel sections having web holes that are edge-stiffened. Fig.1 (b) shows a photograph of a cold-formed steel channel section with an edge-stiffened circular holes (Hawick, 2013). As can be seen, the web holes are stiffened through a continuous edge stiffener/lip around the perimeter of the hole. The study by Yu (2012), while limited to bending, indicates that edge-stiffened holes can significantly improve the strength of cold-formed steel channel sections.



(a) Section with unstiffened holes      (b) Section with edge-stiffened holes

Fig. 1 Cold-formed steel channel sections with web openings

This paper is concerned with the web crippling strength of cold-formed steel channel sections having edge-stiffened circular web holes. Fig.2 shows the definition of symbols used in this paper. While no previous research has considered the web crippling strength of cold-formed steel channel sections with edge-stiffened circular web holes, previous work on web crippling has been reported by Uzzaman *et al.* (2012a, 2012b, 2012c & 2013) and Lian *et al.* (2016a, 2016b, 2017a & 2017b), who proposed design recommendations in the form of web crippling strength reduction factor equations for channel-sections under Two-flanges and One-flange loading conditions. Yu and Davis (1973) and LaBoube *et al.* (1999) also reported research on the web crippling of channel section with unstiffened web openings. For aluminium sections, Zhou and Young (2010) conducted a series of tests and numerical investigation on web

cripling square hollow sections, again with unstiffened web holes. Yousefi *et al.* (2016a,2016b,2017a&2017b) proposed unified strength reduction factor equations for the web crippling strength of cold-formed stainless steel lipped channel-sections with circular web openings.

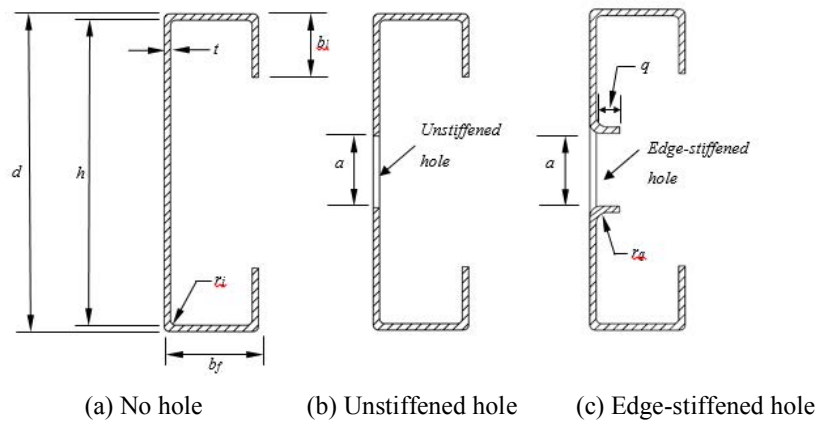


Fig. 2 Definition of symbols

In this paper, a combination of experimental investigation and non-linear elastoplastic finite element analyses (FEA) are used to investigate the effect of edge-stiffened circular web holes on the web crippling strength of lipped channel sections for the interior-one-flange (IOF) and end-one-flange (EOF) loading conditions, as shown in Fig.3 and Fig.4, respectively. The general purpose finite element program ABAQUS (2014) was used for the numerical investigation. A good agreement between the experimental tests and FEA was obtained.

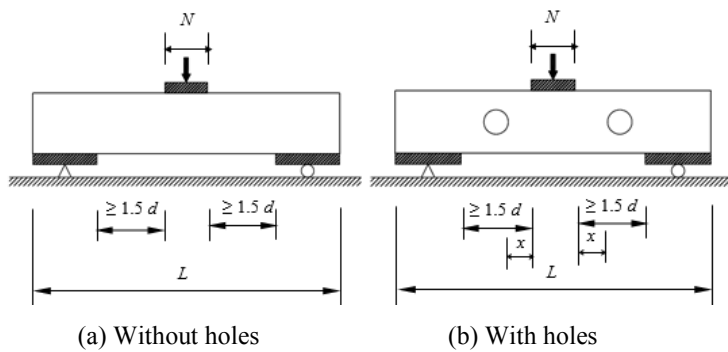


Fig. 3 IOF loading condition with web opening

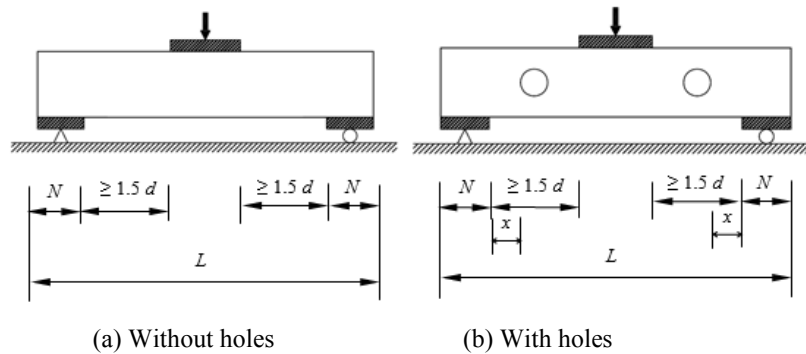


Fig. 4 EOF loading condition with web opening

## 2. Experiment investigation

### 2.1 Test specimens

A test programme was conducted on lipped channel sections, as shown in Fig.2 subjected to web crippling under EOF and IOF loading conditions. Two depths of channel-sections were considered, namely the C240 and C290 channels having the nominal depth of 240mm and 290mm, respectively. All holes had a nominal diameter ( $a$ ) of 140 mm and an edge-stiffener length ( $q$ ) of 13 mm; the radius ( $r_q$ ) between the web and edge-stiffener was 3 mm. The test specimens comprised two different section sizes, having nominal thicknesses ( $t$ ) ranging from 2.0 mm to 2.5 mm; the nominal depth ( $d$ ) of the webs ranged from 240 mm to 290 mm; the nominal flange width ( $b_f$ ) for both sizes is 45 mm.

The test programme considered both webs having unstiffened circular holes and webs having edge-stiffened circular holes. Channel sections with no circular web holes (i.e. plain webs) were also tested, in order that the strength reduction can be determined experimentally. The ratio of the diameter of the circular holes to the depth of the flat portion of the webs ( $a/h$ ) were 0.6 and 0.5 for the C240 and C290 section, respectively. All test specimens were fabricated with the circular web holes located at the mid-depth of the webs and centred above the bearing plates, with a horizontal clear distance to the near edge of the bearing plates ( $x$ ), as shown in Fig.5 and Fig.6 . The specimen lengths ( $L$ ) used were according to the North American Specification (2007) and the AISI Specification (2005). Generally, the distance between bearing plates was set to be 1.5 times the overall depth of the web ( $d$ ) rather than 1.5 times the depth of

the flat portion of the web ( $h$ ), the latter being the minimum specified in the specification. The measured test specimen dimensions for the IOF and EOF loading conditions is detailed in Uzzaman *et al* (2017). The bearing plates were fabricated using with high strength steel having a thickness of 25 mm. Three lengths of bearing plates ( $N$ ) were used: 50 mm, 75 mm and 100 mm.

## 2.2 Test specimens

In Table 2 and Table 3, the specimens were labelled such that the nominal dimension of the specimen, the length of the bearing and the types of holes. For example, the labels “202N50NH” defines the following specimens. The first symbol is the nominal depth of the specimens in millimeters. The notation "N50" indicates the length of bearing in millimeters (50 mm). The last three notations "NH", "USH" and "ESH" indicates the web holes cases. "NH" represents the no web hole case, "USH" represents a web having a hole that is unstiffened, and "ESH" represents a web having a hole that is edge-stiffened.

## 2.3 Material properties

Six coupon tests were carried out to determine the material properties of the channel specimens. The tensile coupons were taken from the centre of the web plate in the longitudinal direction of the untested specimens. The tensile coupons were prepared and tested according to the British Standard for Testing and Materials (2001) for the tensile testing of metals using 12.5 mm wide coupons of a gauge length 50 mm. The coupons were tested in a MTS displacement controlled testing machine using friction grips. Two strain gauges and a calibrated extensometer of 50 mm gauge length were used to measure the longitudinal strain. The material properties obtained from the tensile coupon tests are summarised in

Table 1, which includes the measured static 0.2% proof stress ( $\sigma_{0.2}$ ), and the static tensile strength ( $\sigma_u$ )

	Section	$\sigma_{0.2}$ (MPa)	$\sigma_u$ (MPa)
240x45x15-t1.85	1	264.82	284.78
	2	268.81	283.75
	3	263.39	287.81
290x45x15-t2.5	1	318.92	410.23
	2	328.62	413.31
	3	332.81	414.48

Table 1: Material properties of the specimens

## 2.4 Test rig and procedure

The specimens were tested under the IOF and EOF loading conditions specified in the North American Specification (2007) and the AISI Specification (2005) as shown in Fig.5 and Fig.6. For the IOF loading conditions, two channel sections were used to provide symmetric loading. The specimens were bolted to support blocks at each end of the specimens. A bearing plate was positioned at the mid-length of the specimens. The load was applied through bearing plate. Hinge supports were simulated by two half rounds in the line of action of the force. Two displacement transducers (LVDTs) were positioned at the two edges of bearing plate to measure the vertical displacements. For the EOF loading conditions, two channel specimens were used to provide symmetric loading. The specimens were bolted to a load transfer block at the central loading point. The load was applied through the load transfer plate bolted to the channel sections. Two identical bearing plates of the same width were positioned at both ends of the specimen. Hinge supports were simulated by two half rounds in the line of action of the force. Four displacement transducers (LVDTs) were used to measure the vertical displacements.

A servo-controlled Tinius-Olsen testing machine was used to apply a concentrated compressive force to the test specimens. Displacement control was used to drive the hydraulic actuator at a constant speed of 0.05 mm/min for all the test specimens. The bearing plates were fabricated using a high strength steel. All the bearing plates were machined to specified dimensions, and the thickness was 25 mm. In the experimental investigation, three different lengths of bearing plates ( $N$ ) were used, namely, 50 mm, 75 mm and 100 mm. The flanges of the channel section specimens were unfastened the bearing plates during testing.

## 2.5 Test Results

A total of 36 specimens were tested under IOF and EOF loading conditions. The experimental ultimate web crippling loads per web ( $P_{EXP}$ ) for IOF and EOF loading conditions are given in Table 1 and Table 2, respectively. The typical failure mode of web crippling of the specimens is shown in Fig.7 (a) and Fig.8 (a). A typical example of the load-deflection curve obtained from a specimen both without and with web holes, and the comparisons with the numerical results is shown in Fig. 9 and Fig. 10.

As shown in Table 2, for the IOF loading condition, it is shown that the web crippling strength reduced 12.54% for the specimen 290-N100-USH and 2.83% for the specimen 290-N100-ESH. As shown in Table 3, for the EOF loading

condition, it is shown that the web crippling strength reduced 28.26% for the specimen 240-N100-USH and 1.45% for the specimen 240-N50-ESH.

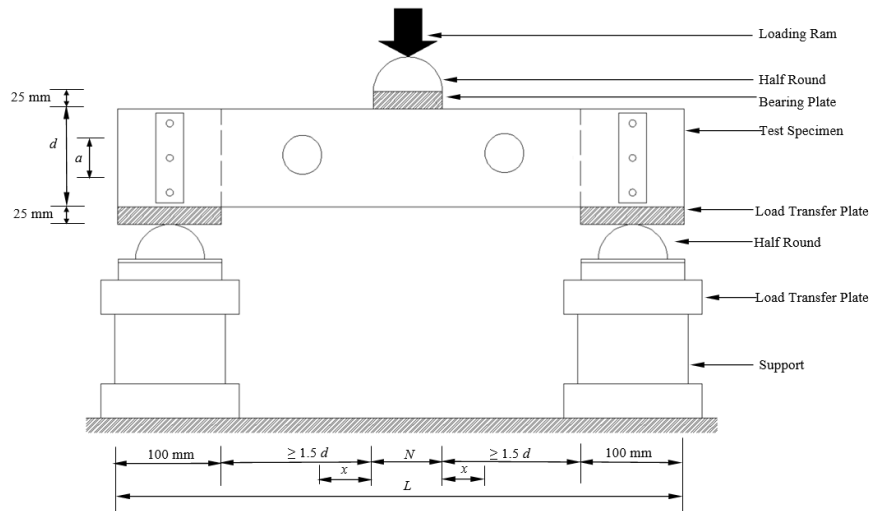


Fig. 5 Schematic view of test set-up for IOF loading condition

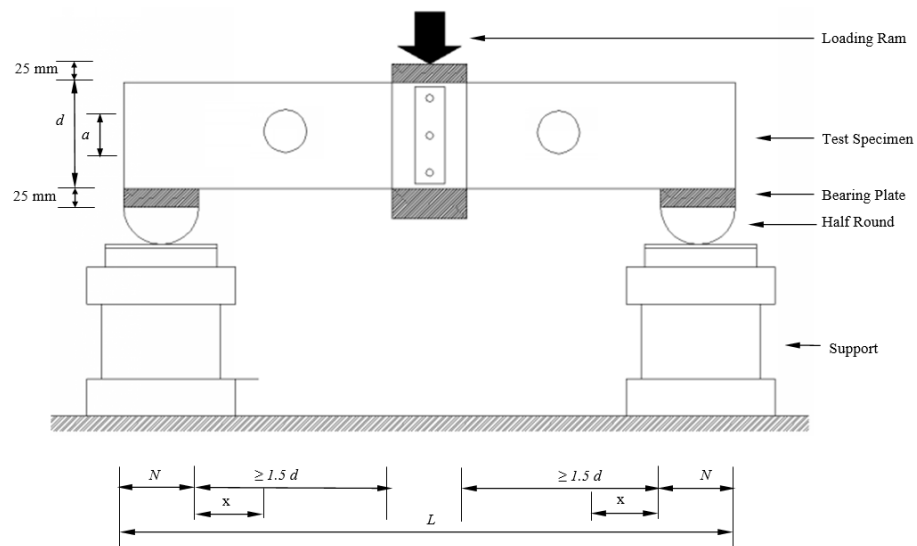


Fig. 6 Schematic view of test set-up for EOF loading condition



### 3. Numerical Investigation

#### 3.1 General

The non-linear elasto-plastic general purpose finite element program ABAQUS (2014) was used to simulate the channel sections with and without holes subjected to web crippling. The bearing plates, the channel section with circular holes and the interfaces between the bearing plates and the channel section have been modelled. In the finite element model, the measured cross-section dimensions and the material properties obtained from the tests were used. The model was based on the centreline dimensions of the cross-sections. Specific modelling issues are described in the following subsection.

#### 3.2 Geometry and material properties

Due to symmetry, only half of the test setup was modelled, as shown in Fig.7 (b) and Fig.8 (b). The dimensions of the channel section modelled are given in detailed in Uzzaman *et al* (2017). Contact pairs are defined between the bearing plate and the cold-formed steel section. In addition, for the IOF loading condition, contact pairs are defined between the support block and cold-formed steel section. For the EOF loading condition, contact pair are defined between the load transfer block and cold-formed steel section. The value of Young's modulus was 205 kN/mm<sup>2</sup> and Poisson's ratio was 0.3. ABAQUS required the material stress-strain curve input as true stress-true plastic strain. The stress-strain curves were directly obtained from the tensile tests and converted into true stress- true plastic strain curves using equations, as specified in the ABAQUS manual (2014),

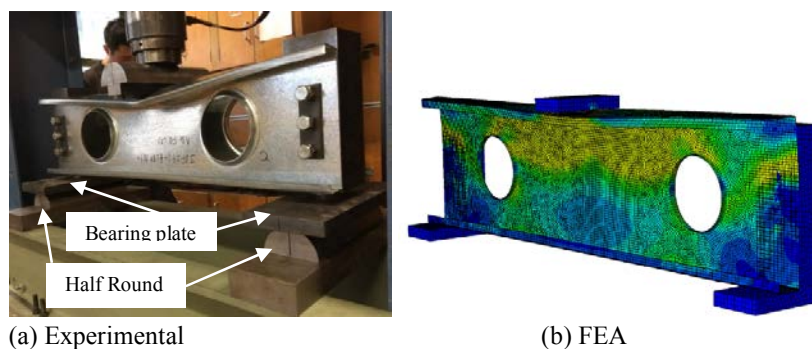


Fig.7 Comparison of experiment and FEA for IOF loading condition.

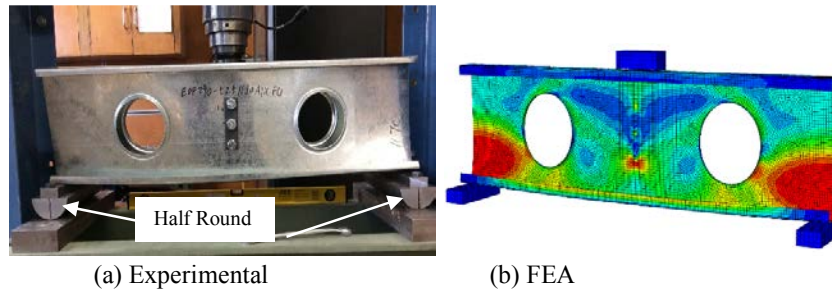


Fig.8 Comparison of experiment and FEA for EOF loading condition.

### 3.3 Element type and mesh sensitivity

Fig.7 (b) and Fig.8 (b) show details of a typical finite element mesh of the channel section, the bearing plate, load transfer block and support block. A mesh sensitivity analysis was used to investigate the effect of different element sizes in the cross-section of the channel sections. Finite element mesh sizes were  $5 \text{ mm} \times 5 \text{ mm}$  for the cold-formed steel channel sections and  $8 \text{ mm} \times 8 \text{ mm}$  for the bearing plates and load transfer block. It is necessary to finely mesh the corners of the section due to the transfer of stress from the flange to the web. From the mesh sensitivity analysis, due to the contact between the bearing plate and inside round corners that form the bend between the flange and web, it was found that at least fifteen elements were required for the corners between the flange and web. On the other hand, for the corners between the flange and lip of the section, only three elements were required. Cold-formed steel channel sections with and without web holes were modelled using S4R shell element. The S4R is a four-node double curved thin or thick shell element with reduced integration and finite membrane strains. It is mentioned in the ABAQUS Manual (2014) that the S4R element is suitable for complex buckling behaviour. The S4R has six degrees of freedom per node and provides accurate solutions to most applications. The bearing plates and load transfer block were modelled using analytical rigid plates and C3D8R element, which is suitable for three-dimensional modelling of structures with plasticity, stress stiffening, large deflection, and large strain capabilities. The solid element is defined by eight nodes having three translational degrees of freedom at each node.

### 3.4 Loading and boundary conditions

The vertical load applied to the channel section through the bearing plate for the IOF and load transfer block for the EOF in the laboratory tests was modelled using displacement control. In the finite element model, a displacement in the

vertical y direction was applied to the reference point of the analytical rigid plate that modelled the bearing plate and load transfer block. The nodes on symmetry surface of load transfer block, support blocks and bearing plates were prevented from translational axes in the x direction and rotation about the y and z axes. The channel section specimens were tested in pairs, which were bolted to load transfer block for the EOF and support blocks for the IOF through the web by a vertical row of M16 high tensile bolts. In the shell element idealisation, cartesian connectors were used to simulate the bolts instead of physically modelling bolts and holes. "CONN3D2" connector elements were used to model the in-plane translational stiffness i.e. y- and z-directions. The stiffness of the connectors element was 10 kN/mm, which Lim and Nethercot (2003, 2004) suggest would be suitable. In the x direction, the nodes were prevented from translating. Contact pair (surface-to-surface) was used to model the interface between the rigid plate (master surface) and the flange of the cross-section (slave surface, extended up to the corners) assuming frictionless response in the tangential direction and hard response in the normal one. For the IOF loading condition, contact pairs were modelled between the support block, bearing plate and cold-formed steel section. For the EOF loading condition, contact pairs were modelled between the load transfer block, bearing plates and cold-formed steel section. All contact surfaces were not allowed to penetrate each other.

### 3.5 Verification of finite element model

In order to validate the finite element model, the experimental failure loads were compared against the failure load predicted by the finite element analysis. The main objective of this comparison was to verify and check the accuracy of the finite element model. A comparison of the test results ( $P_{EXP}$ ) with the numerical results ( $P_{FEA}$ ) of web crippling strengths per web is shown in Table 2 and Table 3 for the IOF and EOF condition, respectively. It can be seen that good agreement has been achieved between both results for all specimens. The mean value of the  $P_{EXP}/P_{FEA}$  ratio is 0.99 and 0.98 with the corresponding coefficient of variation (COV) of 0.02 and 0.01 for the IOF and EOF loading condition, respectively. A maximum difference of 4% and 5% was observed between the experimental and the numerical results for the specimen 290-N100-USH and 240x-N50-USH, respectively. The web deformation curves predicted by finite element analysis were compared with the experimental curves, as shown in Fig.9 and Fig.10 for the IOF and EOF loading conditions, respectively. It is shown that good agreement is achieved between the experimental and finite element results.

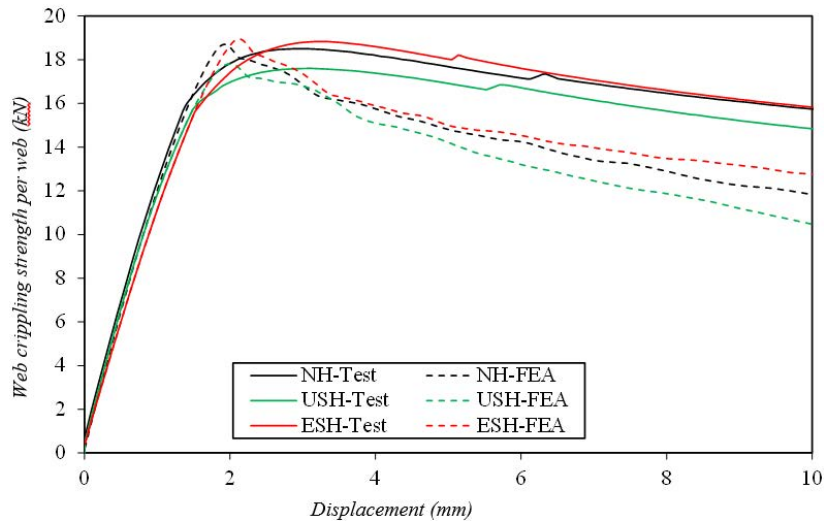


Fig.9 Comparison of web deformation curves for IOF loading condition (Specimens 240-N100).

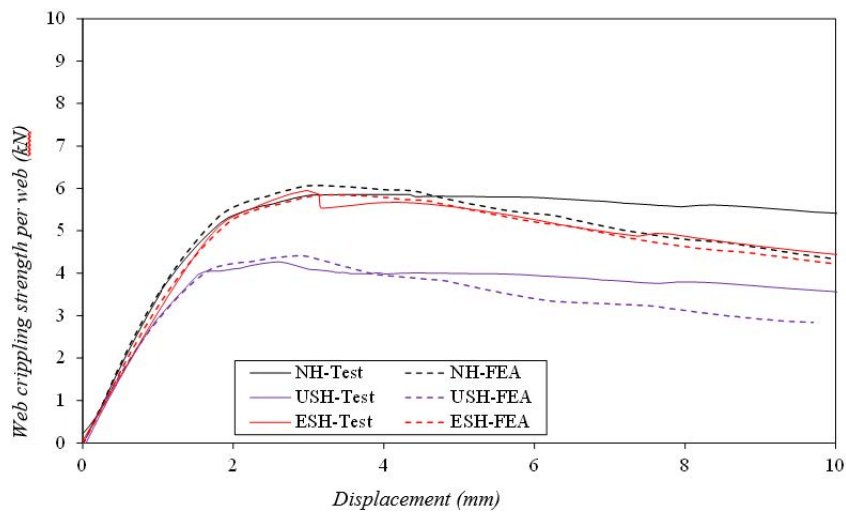


Fig.10 Comparison of web deformation curves for EOF loading condition (Specimens 240-N50)

Specimen	Web slenderness $(h/t)$	Web hole ratio, $(a/h)$ (kN)	Exp. Load per web, $P_{EXP}$ (kN)	Strength reduction due to web holes $R$ (%)	Strength per web predicted from FEA, $P_{FEA}$ (kN)	Comparison, $P_{EXP}/P_{FEA}$
<b>Plain section</b>						
240-N50-NH	118.0	0	16.07	-	16.20	0.99
240-N75-NH	118.9	0	17.3	-	17.50	0.99
240-N100-NH	118.6	0	18.5	-	18.70	0.99
290-N50-NH	114.7	0	30.68	-	31.20	0.98
290-N75-NH	114.8	0	32.97	-	33.89	0.97
290-N100-NH	115.2	0	34.6	-	35.64	0.97
<b>Unstiffened hole</b>						
240-N50-USH	117.4	0.6	15.72	-2.18	15.96	0.98
240-N75-USH	117.5	0.6	16.64	-3.82	16.84	0.99
240-N100-USH	118.2	0.6	17.6	-4.86	17.80	0.99
290-N50-USH	114.8	0.5	28.34	-7.63	29.02	0.98
290-N75-USH	115.3	0.5	29.64	-10.10	30.81	0.96
290-N100-USH	114.9	0.5	30.26	-12.54	32.14	0.94
<b>Edge-stiffened hole</b>						
240-N50-ESH	118.0	0.6	16.26	1.18	16.54	0.98
240-N75-ESH	117.5	0.6	17.54	1.39	17.70	0.99
240-N100-ESH	118.6	0.6	18.83	1.78	18.95	0.99
290-N50-ESH	115.0	0.5	30.07	-1.99	29.87	1.01
290-N75-ESH	115.2	0.5	32.05	-2.79	31.42	1.02
290-N100-ESH	114.2	0.5	33.62	-2.83	33.10	1.02
Mean						0.99
COV						0.02

Table 2: Comparison of the web crippling strength predicted from the finite element analysis with the experimental results for IOF loading.

Specimen	Web slenderness	Web hole ratio,	Exp. Load per web,	Strength reduction due to web holes	Strength per web predicted from FEA,	Comparison,
	(h/t)	(a/h)	$P_{EXP}$ (kN)	R (%)	$P_{FEA}$ (kN)	$PEXP/P_{FEA}$
<b>Plain section</b>						
240-N50-NH	118.5	0	5.82	-	5.81	1.00
240-N75-NH	118.3	0	6.41	-	6.49	0.99
240-N100-NH	117.7	0	6.9	-	7.01	0.98
290-N50-NH	115.5	0	10.5	-	10.65	0.99
290-N75-NH	115.7	0	11.1	-	11.26	0.99
290-N100-NH	115.6	0	11.7	-	11.86	0.99
<b>Unstiffened hole</b>						
240-N50-USH	118.4	0.6	4.22	-27.49	4.42	0.95
240-N75-USH	116.7	0.6	4.6	-28.24	4.80	0.96
240-N100-USH	117.2	0.6	4.95	-28.26	5.16	0.96
290-N50-USH	115.9	0.5	8.4	-20.00	8.72	0.96
290-N75-USH	115.9	0.5	8.95	-19.37	9.34	0.96
290-N100-USH	115.9	0.5	9.48	-18.97	9.86	0.96
<b>Edge-stiffened hole</b>						
240-N50-ESH	118.2	0.6	5.74	-1.37	5.85	0.98
240-N75-ESH	118.2	0.6	6.3	-1.72	6.43	0.98
240-N100-ESH	117.9	0.6	6.8	-1.45	6.86	0.99
290-N50-ESH	114.9	0.5	10.4	-0.95	10.51	0.99
290-N75-ESH	114.7	0.5	10.96	-1.26	11.13	0.98
290-N100-ESH	115.3	0.5	11.52	-1.54	11.78	0.98
Mean					0.98	0.99
COV						0.01

Table 3: comparison of the web crippling strength predicted from the finite element analysis with the experiment results for EOF loading

#### 4. Conclusions

The experimental and the numerical investigations of lipped channel sections with circular unstiffened and edge-stiffened circular web holes subjected to web crippling have been presented. Web holes located at the mid-depth of the web with a horizontal clear distance to the near edge of bearing plate were considered. A series of tests was conducted on lipped channel sections with web holes subjected to the interior-one-flange (IOF) and end-one-flange (EOF) loading conditions. A total of 36 specimens were tested under IOF and EOF loading conditions. The channel specimens had the measured 0.2% proof stresses (yield stresses) of 268 MPa and 328 MPa for the two different section sizes. For the unstiffened hole, it has been shown that for case of specimen 290-N100, the web crippling strength was reduced by 12% for the IOF loading condition. Similarly, for the case of specimen 240-N100, the web crippling strength was reduced by 28% for the EOF loading condition. However, with the edge-stiffened circular hole, the web crippling strength was only reduced by 3% for the IOF loading condition and there was no reduction in strength for the EOF loading condition. A finite element model that incorporated the geometric and the material nonlinearities has been developed and verified against the experimental results. The finite element model was shown to be able to closely predict the web crippling behaviour of the channel sections, both with and without web holes. The new web crippling test data presented in this paper can be used to develop design rules for cold-formed steel sections.

#### Acknowledgements

The Authors would like to acknowledge Howick Ltd. for providing the test specimens. The experimental work was carried out by Wei Lin and Cong Li, as part of their undergraduate research projects. The authors also wish to thank Ross Reichardt and Mark Byrami for their assistance in preparing the specimens and carrying out the experimental testing.

#### Appendix. – References

- ABAQUS. 2014 Version 6.14. RI, USA.: SIMULIA, Providence.
- AISI. 2005 Specification for the design of cold-formed steel structural members. Washington, D.C: American Iron and Steel Institute.
- EN, B. 2001. 10002-1: 2001. Tensile testing of metallic materials. Method of test at ambient temperature. *British Standards Institution*.
- Howick.2013. Floor Joist System. Auckland, New Zealand.
- Laboube, R. A., Yu, W. W., Deshmukh, S. U. & Uphoff, C. A. 1999.Crippling Capacity of Web Elements with Openings. *Journal of Structural Engineering*, 125, 137-141.

- Lian Y, Uzzaman A, Lim JBP, Abdelal G, Nash D, Young B. 2016a. Effect of web holes on web crippling strength of cold-formed steel channel sections under end-one-flange loading condition - Part I: Tests and finite element analysis. *Thin-Walled Structures*, 107, 443-452.
- Lian Y, Uzzaman A, Lim JBP, Abdelal G, Nash D, Young B. 2016b. Effect of web holes on web crippling strength of cold-formed steel channel sections under end-one-flange loading condition - Part II: Parametric study and proposed design equations. *Thin-Walled Structures*, 107, 489-501.
- Lian Y, Uzzaman A, Lim JBP, Abdelal G, Nash D, Young B. 2017a. Web Crippling Behaviour of Cold-Formed Steel Channel Sections with Web Holes Subjected to Interior-One-Flange Loading Condition-Part I: Experimental and Numerical Investigation. *Thin-Walled Structures*, 111, 103-112.
- Lian Y, Uzzaman A, Lim JBP, Abdelal G, Nash D, Young B. 2017b. Web Crippling Behaviour of Cold-Formed Steel Channel Sections with Web Holes Subjected to Interior-One-Flange Loading Condition - Part II: Parametric Study and Proposed Design Equations. *Thin-Walled Structures*, 114, 92-106.
- Lim JBP, Nethercot D. 2003. Finite Element Idealization of a Cold-Formed Steel Portal Frame. *Journal of Structural Engineering*, 130, 78-94.
- Lim JBP, Nethercot DA. 2004. Stiffness prediction for bolted moment-connections between cold-formed steel members. *Journal of Constructional Steel Research*, 60, 85-107.
- NAS 2007. North American Specification for the design of cold-formed steel structural members. Washington, D.C.: American Iron and Steel Institute.
- Rhodes, J. & Nash, D. 1998. An investigation of web crushing behaviour in thin-walled beams. *Thin-Walled Structures*, 32, 207-230.
- Sivakumaran, K. S. & Zielonka, K. M. 1989. Web crippling strength of thin-walled steel members with web opening. *Thin-Walled Structures*, 8, 295-319.
- Uzzaman, A., Lim, J. B. P., Nash, D., Rhodes, J. & Young, B. 2012a. Cold-formed steel sections with web openings subjected to web crippling under two-flange loading conditions—Part I: Tests and finite element analysis. *Thin-Walled Structures*, 56, 38-48.
- Uzzaman, A., Lim, J. B. P., Nash, D., Rhodes, J. & Young, B. 2012b. Cold-formed steel sections with web openings subjected to web crippling under two-flange loading conditions—Part II: Parametric study and proposed design equations. *Thin-Walled Structures*, 56, 79-87.
- Uzzaman, A., Lim, J. B. P., Nash, D., Rhodes, J. & Young, B. 2012c. Web crippling behaviour of cold-formed steel channel sections with offset



- web holes subjected to interior-two-flange loading. *Thin-Walled Structures*, 50, 76-86.
- Uzzaman A, Lim JBP, Nash D, Rhodes J, Young B. 2013. Effect of offset web holes on web crippling strength of cold-formed steel channel sections under end-two-flange loading condition. *Thin-Walled Structures*, 65, 34-48.
- Uzzaman A, Lim JBP, Nash D, Rhodes J, Young B. 2017. Effects of edge-stiffened circular holes on the web crippling strength of cold-formed steel channel sections under one-flange loading conditions. *Thin-Walled Structures*, 139, 96-107.
- Yousefi A, Lim JBP, Uzzaman A, Lian Y, Clifton C, Young B. 2016a. Web crippling strength of cold-formed stainless steel lipped channel-sections with web openings subjected to Interior-One-Flange loading condition. *Steel and composite structures*. 21(3), 629-659.
- Yousefi A, Lim JBP, Uzzaman A, Lian Y, Clifton C, Young B. 2016b. Design of cold-formed stainless steel lipped channel-sections with web openings subjected to web crippling under End-One-Flange loading condition. *Advances in Structural Engineering*. 20(7), 1024-1045.
- Yousefi A, Uzzaman A, Lim JBP, Clifton C, Young B. 2017a. Numerical investigation of web crippling strength in cold-formed stainless steel lipped channels with web openings subjected to interior-two-flange loading condition. *Steel and composite structures*. 23 (4), 363-38
- Yousefi A, Uzzaman A, Lim JBP, Clifton C, Young B. 2017b. Web crippling strength of cold-formed stainless steel lipped channels with web perforations under end-two-flange loading. *Advances in Structural Engineering*, 20(12), 1845-1863.
- Yu C. 2012. Cold-formed steel flexural member with edge stiffened holes: Behavior, optimization, and design. *Journal of Constructional Steel Research*, 71, 210-8.
- Yu, W. W. & Davis, C. S. 1973. Cold-formed steel members with perforated elements. *Journal of the Structural Division*, 99, 2061-2077.
- Zhou, F. & Young, B. 2010. Web crippling of aluminium tubes with perforated webs. *Engineering Structures*, 32, 1397-1410.